Mineralogical Magazine (2019), **83**, 733–739
doi:10.1180/mgm.2019.45

CAMBRIDGE UNIVERSITY PRESS

Article

Hitachiite, $Pb_5Bi_2Te_2S_6$, a new mineral from the Hitachi mine, Ibaraki Prefecture, Japan

Takahiro Kuribayashi[1]*, Toshiro Nagase[2], Tatsuo Nozaki[3,4,5,6], Junichiro Ishibashi[7], Kazuhiko Shimada[7], Masaaki Shimizu[8] and Koichi Momma[9]

[1]Department of Earth Science, Graduate School of Science, Tohoku University, Sendai 980-8578, Japan; [2]The Tohoku University Museum, Tohoku University, Sendai 980-8578, Japan; [3]Research and Development Centre for Submarine Resources, Japan Agency for Marine-Earth Science and Technology, Yokosuka, 237-0061, Japan; [4]Frontier Research Centre for Energy and Resources, School of Engineering, The University of Tokyo, Tokyo 113-8656, Japan; [5]Department of Planetology, Kobe University, Kobe 657-8501, Japan; [6]Ocean Resources Research Centre for Next Generation, Chiba Institute of Technology, Narashino 275-0016, Japan; [7]Department of Earth and Planetary Sciences, Faculty of Science, Kyushu University, Fukuoka 819-0395, Japan; [8]Department of Earth System Science, Graduate School of Science and Engineering for Education, University of Toyama, Toyama 930-8555, Japan; and [9]Department of Geology and Paleontology, National Museum of Nature and Science, Tsukuba 305-0005, Japan.

Abstract

Hitachiite, $Pb_5Bi_2Te_2S_6$, is a new mineral discovered in the Hitachi mine, located in the Ibaraki Prefecture of Japan. The mean of 21 electron microprobe analyses gave: Pb 52.01, Bi 23.06, Fe 0.69, Sb 0.17, Te 13.74, S 9.71, Se 0.54, total 100.04 wt.%. The empirical chemical formula based on 15 apfu is $(Pb_{4.75}Fe_{0.23})_{\Sigma 4.98}(Bi_{2.09}Sb_{0.03})_{\Sigma 2.12}Te_{2.04}(S_{5.73}Se_{0.13})_{\Sigma 5.86}$, ideally $Pb_5Bi_2Te_2S_6$. Synchrotron single-crystal X-ray diffraction experiments indicated that hitachiite has trigonal symmetry, space group $P\bar{3}m1$, with $a = 4.2200(13)$ Å, $c = 27.02(4)$ Å and $Z = 1$. The four strongest diffraction peaks shown in the powder X-ray pattern [*d*, Å (*I*)(*hkl*)] are: 3.541(35)(012), 3.391(59)(013), 3.039(100)(015) and 2.114(56)(110). The calculated density (D_{calc}) for the empirical chemical formula is 7.54 g/cm^3.

The crystal structure of hitachiite has been refined using synchrotron single-crystal X-ray diffraction data, to $R = 7.38\%$ and is based on *ABC*-type stacking of 15 layers (five Pb, two Bi, two Te, and six S layers) along the [001] direction, and with each layer ideally containing only one kind of atom. The stacking sequence is described as Te–Bi–S–Pb–S–Pb–S–Pb–S–Pb–S–Pb–S–Bi–Te. The discovery of hitachiite implies that the minerals of the Bi_2Te_2S–PbS join might form a homologous series of $Bi_2Te_2S{\cdot}n$PbS.

Keywords: hitachiite, new mineral, tetradymite group minerals, homologous series

(Received 28 February 2019; accepted 6 July 2019; Accepted Manuscript published online: 15 July 2019; Associate Editor: František Laufek)

Introduction

Hitachiite, $Pb_5Bi_2Te_2S_6$, is a new mineral discovered in the Hitachi mine, Ibaraki Prefecture, Japan. The chemical formula of hitachiite is plotted on the join of Bi_2Te_2S (tetradymite)–PbS (galena) in the system Bi–Pb–(Te, S). The join also includes aleksite ($PbBi_2Te_2S_2$) and saddlebackite ($Pb_2Bi_2Te_2S_3$), which belong to the tetradymite group of minerals in the 9th edition of the Strunz mineral classification system (Strunz and Nickel, 2001). The mineral and its name have been approved by the Commission on New Minerals, Nomenclature and Classification of the International Mineralogical Association (IMA2018-027, Kuribayashi *et al.*, 2018). The type specimen of hitachiite is deposited under catalogue number NSM-M45821 in the National Museum of Nature and Science, Tsukuba, Ibaraki Prefecture, Japan.

The crystal structures of the tetradymite group of minerals can be considered as combinations of several structural units. Bindi and Cipriani (2003) investigated Pb-enriched baksanite $(Bi_5Pb)Te_2S_3$; baksanite, $Bi_6Te_2S_3$, is one of the tetradymite group of minerals), and reported that its crystal structure can be described as an alternation of modules of an ingodite-type structure (Bi_2TeS) and of a joséite-A-type structure (Bi_4TeS_2). Similarly, hitachiite can be considered as a homologous series of $Pb_nBi_4Te_4S_{n+2}$ in the Pb–Bi tellurosulfides proposed by Cook *et al.* (2007*a*,*b*). The general formula has been reviewed by Moëlo *et al.* (2008) as $Pb_{(n-1)}Bi_2Ch_{(n+2)}$ (*Ch* = Te, Se and S) on the basis of the tetradymite archetype. It is therefore important to determine the crystal structure of hitachiite in order to classify it in the tetradymite group of minerals. The discovery of hitachiite presents the possibility of forming a homologous series with aleksite and saddlebackite, expressed as $Bi_2Te_2S{\cdot}n$PbS. As the crystal structures of aleksite and saddlebackite have not been determined so far, determining the structure of hitachiite could help in understanding the structural and crystal chemistry of minerals in the system Bi_2Te_2S–PbS. In this report, we present the structure of hitachiite refined using single-crystal synchrotron X-ray diffraction data.

Occurrence and appearance

Hitachiite was discovered at the Hitachi mine, located in the city of Hitachi, Ibaraki Prefecture, Japan (36°37′16.03″N, 140°36′46.50″E). The Hitachi mine comprises Fudotaki and Fujimi deposit groups,

*Author for correspondence: T. Kuribayashi, Email: takahiro.kuribayashi.a7@tohoku.ac.jp
Cite this article: Kuribayashi T., Nagase T., Nozaki T., Ishibashi J., Shimada K., Shimizu M. and Momma K. (2019) Hitachiite, $Pb_5Bi_2Te_2S_6$, a new mineral from the Hitachi mine, Ibaraki Prefecture, Japan. *Mineralogical Magazine* **83**, 733–739. https://doi.org/10.1180/mgm.2019.45

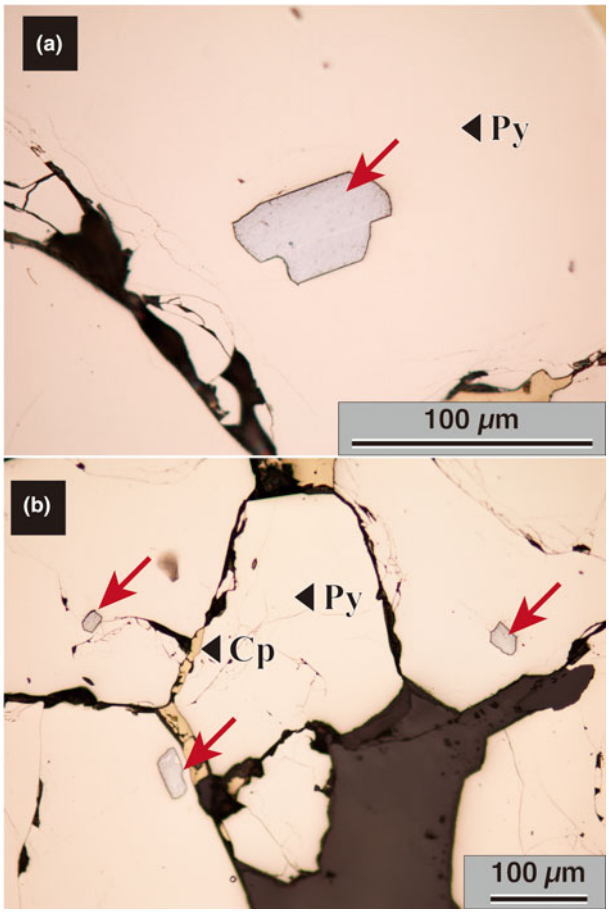

Fig. 1. Optical reflected light microscopy images of hitachiite: (*a*) magnified image of a hitachiite grain; and (*b*) hitachiite found commonly in pyrite. Holotype specimen, catalogue number NSM-M45821.

with the aforementioned Fudotaki deposit being one of the representative orebodies of the Fudotaki group (Kase and Yamamoto, 1985). The Fudotaki deposit is classified as a volcanogenic massive sulfide (VMS) deposit and a Cu–Zn sulfide deposit with small amounts of Pb. The Fudotaki sulfide ores have been metamorphosed into lower epidote–amphibole facies via regional metamorphism. The primary formation age of the Fudotaki deposit was estimated to have been formed during the Cambrian period. The Fudotaki deposit is recognised as the oldest dated ore deposit in Japan by both zircon U–Pb radiometric determinations and Re–Os isotope isochron methods (Tagiri *et al.*, 2011; Nozaki *et al.* 2014).

Emeritus Prof. K. Kase of Okayama University collected samples (including hitachiite) from the Fudotaki deposit at Hitachi mine to investigate geochemically its mineralisation and metallogenesis (Kase, 1978; Kase and Yamamoto, 1985). Hitachiite crystals occur as tiny grains within pyrite crystals (Fig. 1*a*,*b*) and are commonly found with pyrite, chalcopyrite, minor amounts of sphalerite and pyrrhotite and very minor amounts of galena and marcasite. The individual grains are ~10–100 μm in size.

Optical and physical properties

The polished section including abundant hitachiite crystals were made using the type specimen with catalogue number NSM-M45821. Hitachiite is an opaque mineral with a metallic lustre and black streak. The macroscopic colour of hitachiite is silver grey. Polished specimens of hitachiite reveal that its bireflectance is weak with no observable pleochroism; its anisotropy is weak and no internal reflections are shown. Hitachiite has a Mohs' hardness of 2½–3. Its calculated density is 7.54 g/cm^3 when using the empirical chemical formula and structural data ($Z = 1$).

Table 1. Reflectance data (R_1 and R_2 in %) in air and oil of hitachiite.

	Air		Oil	
λ (nm)	R_1	R_2	R_1	R_2
400	38.4	35.8	30.3	25.1
420	40.0	36.3	30.4	25.9
440	41.6	37.4	30.4	26.8
460	41.7	38.3	30.3	27.4
470	**41.8**	**38.5**	**30.2**	**27.7**
480	41.9	38.7	30.0	27.8
500	41.8	39.0	29.7	28.0
520	41.7	38.9	29.3	28.1
540	41.6	38.9	29.3	28.1
546	**41.5**	**38.8**	**29.0**	**28.0**
560	41.4	38.7	28.8	27.9
580	41.2	38.6	28.7	27.9
589	**41.1**	**38.4**	**28.4**	**28.2**
600	41.1	38.1	28.4	28.2
620	40.8	38.1	28.3	28.2
640	40.8	38.1	28.3	28.2
650	**40.7**	**38.1**	**28.3**	**28.3**
660	40.7	38.0	28.2	28.4
680	40.6	37.8	28.1	28.4
700	40.3	37.5	27.9	28.4

The values required by the Commission on Ore Mineralogy are given in bold.

Reflectance data

After optical observations, reflectance measurements were conducted on selected hitachiite crystals within the polished section. Reflectance measurements for hitachiite were performed against a WC009 standard material, which had been measured relative to a WTiC (Zeiss 314) by the late A.J. Criddle. Immersion measurements were performed using Nikon oil ($N_D = 1.515$) at room temperature (20°C). A Nikon Optiphot-2 microscope photometer with a Nikon photometer-head-measurement-finder, a Nikon photometer controller P101, a Nikon monochromator G-70 and a Nikon two-light-flux interference examination installed at the University of Toyama were used for these measurements. The reflectance data are summarised in Table 1

Chemical data

The composition of hitachiite was obtained using a field emission electron probe micro-analyser (JEOL, JXA-8530F) at Kyushu University, under operating conditions of 20 kV and 10 nA with a beam diameter of 0.1 μm. Counting time was set at 40 s for each element. Standard materials used to quantitatively analyse the samples were: galena for Pb; bismuthinite for Bi; Sb_2Te_3 for Te; pyrite for Fe and S; stibnite for Sb; and In_2Se_3 for Se. The measured X-ray intensities were corrected using the *ZAF* method. Although the compositions of some samples are slightly different, no chemical zoning was observed in hitachiite grains (Fig. 2). One-point analysis was conducted per hitachiite crystal within the polished section used for optical observation and reflectance measurement,

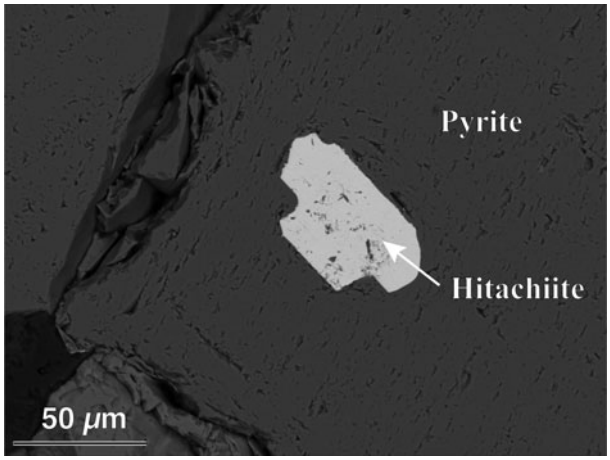

Fig. 2. Back-scattered electron image of a hitachiite grain. Holotype specimen, catalogue number NSM-M45821.

and the results of 21 analyses are summarised in Supplementary Table S1 (see below); these results yield hitachiite's empirical formula of $(Pb_{4.75}Fe_{0.23})_{\Sigma 4.98}(Bi_{2.09}Sb_{0.03})_{\Sigma 2.12}Te_{2.04}(S_{5.73}Se_{0.13})_{\Sigma 5.86}$ based on 15 atoms per formula unit. The ideal chemical formula for hitachiite is $Pb_5Bi_2Te_2S_6$. The chemical formula of hitachiite lies on the join of Bi_2Te_2S–PbS (Fig. 3*a*).

Crystallography

The powder X-ray diffraction (PXRD) pattern of hitachiite was obtained using a Gandolfi camera with a diameter of 114.6 mm and Ni-filtered Cu*K*α radiation (λ = 1.54187 Å) installed at the National Museum of Nature and Science. The data were recorded on an imaging plate and processed through a Fuji BAS-2500 bio-image analyser using computer software written by Nakamuta (1999). The sample used for the PXRD experiment was the same as that used for single-crystal XRD experiment. The PXRD profile of hitachiite and its peak information are shown in Supplementary Fig. S1 and Table 2, respectively. The four strongest diffraction peaks shown in the powder X-ray pattern [*d*, in Å, ($I_{rel.}$), (*hkl*)] are: 3.541 (35) (012), 3.391 (59) (013), 3.039 (100) (015) and 2.114 (56) (110). The diffraction positions were calibrated using silicon as an internal standard. The reflections were indexed by reference to simulated patterns based on the refined crystal structure. The lattice parameters obtained from PXRD are $a = 4.2292(12)$ Å, $c = 27.069(8)$ Å and $V = 419.3(3)$ Å^3.

Single-crystal XRD experiments were conducted using an automated four-circle X-ray diffractometer with synchrotron radiation at the beam line BL-10A, Photon Factory, High Energy Accelerator Research Organisation, KEK, Japan. The wavelength (λ = 0.70134 Å) of synchrotron radiation was calibrated using the obtained unit-cell volume of the ruby standard material (NIST-SRM-1990). In the X-ray oscillation photographs, most of the samples showed diffused and/or streak reflections due to its structural stacking sequence, therefore, a fragment of hitachiite was selected carefully to determine the crystal structure (Fig. 4). The dimension of the sample is ~0.05 mm × 0.02 mm × 0.02 mm, with a chemical formula of $(Pb_{4.60}Fe_{0.25})_{\Sigma 4.85}(Bi_{2.24}Sb_{0.02})_{\Sigma 2.26}Te_{2.15}(S_{5.62}Se_{0.13})_{\Sigma 5.75}$ (No. 5-2 in Table S1). The lattice parameters were determined as follows: $a = 4.2200(13)$ Å, $c = 27.02(4)$ Å and $V = 416.7(7)$ Å^3, based on the 80 centred reflections in the 2θ range 19.1–36.4°. These values are in good agreement with those obtained by PXRD. The X-ray diffraction intensity data were collected up to $2\theta_{max} = 60°$ using a scintillation type detector. Double the unique reciprocal region was measured to check the Laue group. The intensity distribution indicates characteristics of the Laue group $\bar{3}m1$. The absorption coefficient (μ) of the hitachiite sample is 71.7 mm^{-1}. Refdelf type absorption correction (*XABS2*; Parkin *et al.*, 1995) was applied to our dataset using the *WinGX* software (Farrugia, 1999). The value of R_{int} was decreased from 10.8% to 8.6% after the correction. As no systematic absences were observed in the measured intensities, the space group of hitachiite was expected to be $P\bar{3}m1$, $P3m1$ or $P321$. The crystal structure of hitachiite was solved against these space groups via the charge-flipping method (Oszlanyi and Suto, 2004) using the *SUPERFLIP* software (Palatinus and Chapuis, 2007). As a result, the $P\bar{3}m1$ structural

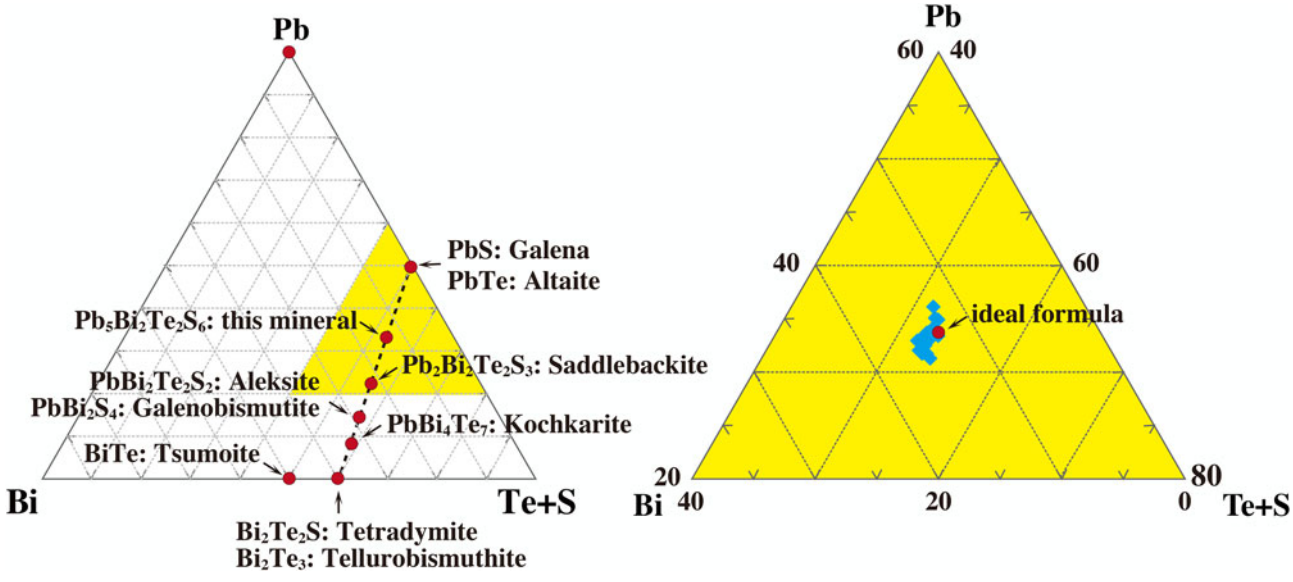

Fig. 3. Chemical properties of hitachiite and related minerals: (*a*) the minerals on the tetradymite–galena join in the system Pb–Bi–(Te + S); and (*b*) the compositional variation of hitachiite (shown by the blue area).

Table 2. Powder X-ray data with normalised (*d* in Å) and calculated intensity of hitachiite.

I_{obs}	I_{calc}	d_{obs} (Å)	d_{calc} (Å)	*h k l*
	0.2		27.031	0 0 1
	0.1		13.515	0 0 2
	0.5		9.010	0 0 3
	0.8		6.758	0 0 4
	1.3		5.406	0 0 5
	1.8		4.505	0 0 6
3	3.0	3.872	3.862	0 0 7
	0.3		3.655	0 1 0
4	2.9	3.635	3.623	0 1 1
35	**22.5**	**3.541**	**3.529**	**0 1 2**
59	**38.3, 16.2**	**3.391**	**3.387, 3.379**	**0 1 3, 0 0 8**
4	6.2	3.222	3.215	0 1 4
100	**100.0**	**3.039**	**3.028**	**0 1 5**
	0.2		3.003	0 0 9
6	10.4	2.839	2.839	0 1 6
	0.4		2.703	0 0 10
2	1.3	2.658	2.655	0 1 7
3	2.0	2.483	2.481	0 1 8
	0.4		2.457	0 0 11
3	3.6	2.323	2.321	0 1 9
	0.3		2.253	0 0 12
14	**17.6**	**2.177**	**2.173**	**0 1 10**
56	**42.7**	**2.114**	**2.111**	**1 1 0**
	0.0		2.104	1 1 1
	0.0		2.085	1 1 2
	0.3		2.079	0 0 13
	0.0		2.055	1 1 3
11	16.1	2.040	2.039	0 1 11
	0.2		2.015	1 1 4
	0.5		1.966	1 1 5
	0.3		1.931	0 0 14
13*	1.1	1.920	1.918	0 1 12
	1.1		1.911	1 1 6
2	2.3	1.856	1.852	1 1 7
	0.0		1.828	0 2 0
	0.4		1.824	0 2 1
9	3.3, 7.0	1.812	1.811, 1.807	0 2 2, 0 1 13
	0.6		1.802	0 0 15
18	6.0, 15.1	1.793	1.791, 1.79	0 2 3, 1 1 8
	1.0		1.764	0 2 4
18	17.4	1.735	1.731	0 2 5
	0.3		1.727	1 1 9
	1.3		1.707	0 1 14
7	1.9, 5.3	1.692	1.694, 1.689	0 2 6, 0 0 16
	0.5		1.664	1 1 10
	0.3		1.652	0 2 7
	0.4		1.616	0 1 15
	0.5		1.608	0 2 8
	0.6		1.601	1 1 11
	0.1		1.590	0 0 17
	0.9		1.561	0 2 9

*This diffraction peak was overlapped with peaks of pyrite. Theoretical powder data are calculated on the basis of the structural model refined by single-crystal X-ray diffraction analysis using a four-circle diffractometer.

model was shown to be eventually most suitable. The atom positions were obtained by inspecting the electron density distributions, and three Pb, one Bi, one Te and three S sites being assigned. The site for the Bi atom was assigned to form a Te–Bi–S stacking sequence, with reference to the possible sequence of several synthesised phases as proposed by Liu and Chang (1994) and Cook *et al.* (2007*a*,*b*). The neutral X-ray scattering factors taken from the *International Tables for Crystallography Volume C* (Prince, 2004) were applied in the structure refinement. As distinguishing between Pb and Bi is difficult owing to their similar scattering factors, the metal sites were considered to be

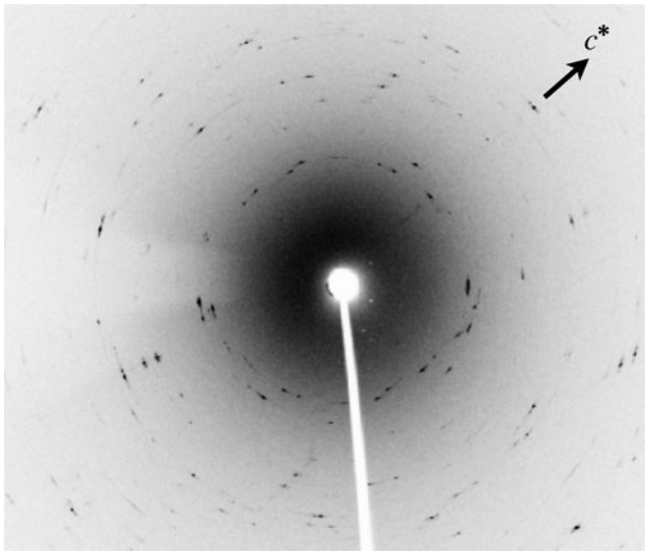

Fig. 4. X-ray oscillation photo of hitachiite taken using synchrotron X-ray radiation with imaging plate. The oscillation angle is ~10°.

occupied by one kind of atom (Pb or Bi). Based on the chemical formula of the examined sample, we considered that a small amount of Fe, Sb and Se were accommodated at Pb, Bi and S sites, respectively. Excess contents of Bi and Te were also divided into Pb and S sites, respectively. Anisotropic displacement factors were applied to Pb and Bi sites, whereas isotropic displacement factors were applied to Te and S sites. An additional site in the interlayer of Te–Te was found after performing a difference-Fourier calculation of the examined sample; this additional site was designated as the TeB site. TeA and TeB sites were too close to be occupied simultaneously. Constraints for the site occupancy and the isotropic displacement factor were applied to these sites as follows: (1) the summation of the occupancy of TeA and TeB is equal to 1; (2) U_{TeA} is equal to U_{TeB}. As this TeB site and another set of residual peaks could be caused by poor crystal quality, such as stacking faults due to chemical variation, we considered that the ideal structure of hitachiite may not possess this site. The residual *R* value was converged to 9.76% (no absorption correction). After the *XABS2* absorption correction, it was improved to 7.38%. All calculations of our structural refinements were performed using *SHELXL97* (Sheldrick and Schneider, 1997) with *WinGX* crystallographic software (Farrugia, 1999). The calculated powder X-ray intensities obtained from this structural model are in good agreement with the measured data (Table 2). Miscellaneous information on data collections are summarised in Table 3 and the final atomic coordinates and anisotropic displacement factors are listed in Table 4. Information on selected interatomic distances in the hitachiite structure are summarised in Table 5. Drawings of each structure were produced using *VESTA 3* (Momma and Izumi, 2011). The crystallographic information files have been deposited with the Principal Editor of *Mineralogical Magazine* and are available with the Supplementary material.

Crystal structure and its relation to other known phases

The ideal composition of hitachiite is $Pb_5Bi_2Te_2S_6$ and it could be regarded as $(Pb_5Bi_2)_{\Sigma 7}(Te_2S_6)_{\Sigma 8}$, which corresponds to the tetradymite group (2.DC.05) in the 9th edition of the Strunz mineral

Table 3. Detailed information on data collection and structural refinement.

Crystal data	
Ideal formula	$Pb_5Bi_2Te_2S_6$
Crystal dimensions (mm)	0.05 × 0.02 × 0.02
Crystal system, space group	Trigonal, $P\bar{3}m1$
Unit-cell dimensions (Å)	a = 4.2200(13), c = 27.02(4)
Unit-cell volume (Å^3)	416.7(7)
Z	1
D_{calc} (g·cm^{-1})	7.54
Temperature (K)	298
Absorption coefficient (mm^{-1})	71.7
Data collection	
Radiation type, wavelength (Å)	Synchrotron, λ = 0.70134 Å
2θmax (°)	60
Absorption correction	*XABS2* (Parkin *et al.*, 1995)
Reflections measured, independent and observed reflections ($I > 2\sigma(I)$)	1993, 246, 724
Structure solution	*SuperFlip* (Palatinus and Chapuis, 2007)
Refinement	
Refinement method	*SHELXL97* (Sheldrick and Schneider, 1997)
Indices range of h, k, l	$-5 \le h \le 5$, $0 \le k \le 6$, $-37 \le l \le 37$
Weighting scheme	$w = 1/[\sigma^2(Fo^2)]$
No. of variables	22
Reflection/Parameters ratio	11.18
R_{int} (%)	10.8
Residuals: $R1$ (%), R (all) (%)	7.38, 8.30
Residuals: $wR2$ (%)	16.29
GoF	0.977
$\Delta\rho_{max}$, $\Delta\rho_{min}$ (e^- Å^{-3})	9.454, −4.413

classification system (Strunz and Nickel, 2001). Makovicky (2006) summarised the crystal structures of sulfide and related chalcogenide compounds. In his summary, the tetradymite series especially, is expressed chemically as the extended selenides and tellurides of bismuth based on the structural classification of Bayliss (1991). The fundamental structural unit of the tetradymite structure has an octahedral double layer Bi_2X_3 (X = Te, Se and S). Considering the high amount of Pb in the chemical formula of hitachiite, it seems to be similar to the lillianite ($Pb_3Bi_2S_6$) series in 2.JA.20 and/or the galenobismutite ($PbBi_2S_4$) series in 2.JA.25 of sulfosalts (Strunz and Nickel, 2001). However, the crystal structure of hitachiite is definitely different from those of lillianite and galenobismutite, and so it cannot be classified to these groups.

The crystal structure of hitachiite is based on *ABC*-type close-packing of each single element atomic sheet stacked along the *c* axis and can be regarded as a layered structure (tetradymite archetype) with a periodicity of ~27 Å. The crystal structure of hitachiite has five Pb, two Bi, two Te and six S sheets. There are three Pb, one Bi, one Te and three S crystallographic sites. The stacking sequence can be expressed as Te–Bi–S–Pb–S–Pb–S–Pb–S–Pb–S–Bi–Te (Fig. 5). The crystal structure of hitachiite contains PbS_6 and $BiTe_3S_3$ octahedra. Its crystal structure can be viewed as composed from a galena and tetradymite unit (Bi_2Te_2S) (Figs 5 and 6). The mean Pb–S and Bi–(Te, S) distances in each octahedron are 2.958(14) Å for Pb1–S, 2.970(16) Å for Pb2–S, 2.974(14) Å for Pb3–S and 3.027(11) Å for Bi–(Te, S). These values are in good agreement with those observed in tetradymite (3.058 Å for Bi–S and 3.129 Å for Bi–Te; Harker *et al.*, 1934) and that in galena (2.9658(8) Å for Pb–S; Noda *et al.*, 1987). Also, the TeA–TeA interlayer distance is 3.773(9) Å and is consistent to those of tetradymite (3.697 Å for Te–Te, Harker *et al.*, 1934; 3.895–4.037 Å for Te–Te and Te–S, Pauling, 1975) and the reported distance (3.65–3.70 Å for Te–Te) by Makovicky (2006).

Table 5. Selected bond distances (Å) in hitachiite with several reference data.

Hitachiite (this study)		Related minerals	
		Galena*	
Pb1 octahedron		Pb octahedron	
Pb1–S2 [x6]	2.958(14)	Pb–S [x6]	2.9658
Pb2 octahedron			
Pb2–S3 [x3]	2.938(17)		
Pb2–S1 [x3]	3.001(14)		
<Pb2–S>	2.970(16)		
Pb3 octahedron			
Pb3–S1 [x3]	2.953(13)		
Pb3–S2 [x3]	2.994(15)		
<Pb3–S>	2.974(14)		
		Tetradymite**	
Bi octahedron		Bi octahedron	
Bi–S3 [x3]	3.028(18)	Bi–S [x3]	3.058
Bi–TeA [x3]	3.025(4)	Bi–Te [x3]	3.129
<Bi–S/Te>	3.027(11)	<Bi–S/Te>	3.094
Interlayer		Interlayer	
TeA–TeA	3.773(9)	Te–Te	3.697

*Data from Noda *et al.* (1987); **Data from Harker *et al.* (1934)

In comparison with the tsumoite (BiTe; $P\bar{3}m1$; Shimazaki and Ozawa, 1978) and the Pb-rich baksanite ($Bi_5PbTe_2S_3$; $P\bar{3}m1$; Bindi and Cipriani, 2003) structures, hitachiite and tetradymite (Bi_2Te_2S; $R\bar{3}$; Harker *et al.*, 1934) structures lack the Bi–Bi double layer (Fig. 5). As shown by Nakajima (1963), in selenides and tellurides of bismuth, there are four species with the tetradymite archetype structure as $Bi_2Te_xSe_{3-x}$ (x = 0, 1, 2 and 3). In contrast, Kuznetsov and Kanishcheva (1970) showed that the compositional limit of tetradymite in the system Bi_2Te_3–Bi_2S_3 was Bi_2STe_2–$Bi_2S_{1.3}Te_{1.7}$. Considering the Te–S substitution, Pauling (1975) suggested that a partial Te–S interlayer could be allowed in the tetradymite structure. In order to form the tetradymite archetype structure, it is key to have tetradymite unit (S–Bi–Te–

Table 4. Final atomic coordinates and displacement factors for hitachiite.

	x	y	z	Occ.	U_{eq} / U_{iso}	U^{11}	U^{22}	U^{33}	U^{23}	U^{13}	U^{12}
Pb1	0	0	½	1	0.0127(13)	0.015(2)	0.015(2)	0.009(4)	0.0000	0.0000	0.0074(11)
Pb2	⅓	⅔	0.24690(13)	1	0.0155(10)	0.0134(17)	0.0134(17)	0.020(3)	0.0000	0.0000	0.0067(9)
Pb3	⅔	⅓	0.37352(14)	1	0.0155(10)	0.0145(18)	0.0145(18)	0.018(3)	0.0000	0.0000	0.0072(9)
Bi	0	0	0.11964(15)	1	0.0196(12)	0.0170(16)	0.0170(16)	0.025(3)	0.0000	0.0000	0.0085(8)
S1	0	0	0.3118(8)	1	0.012(6)*						
S2	⅓	⅔	0.4380(9)	1	0.008(4)*						
S3	⅔	⅓	0.1862(11)	1	0.024(7)*						
TeA	⅓	⅔	0.0533(2)	0.81(2)	0.0032(16)*						
TeB	⅓	⅔	0.0044(10)	0.19(2)	0.0032(16)*						

* U_{iso}.

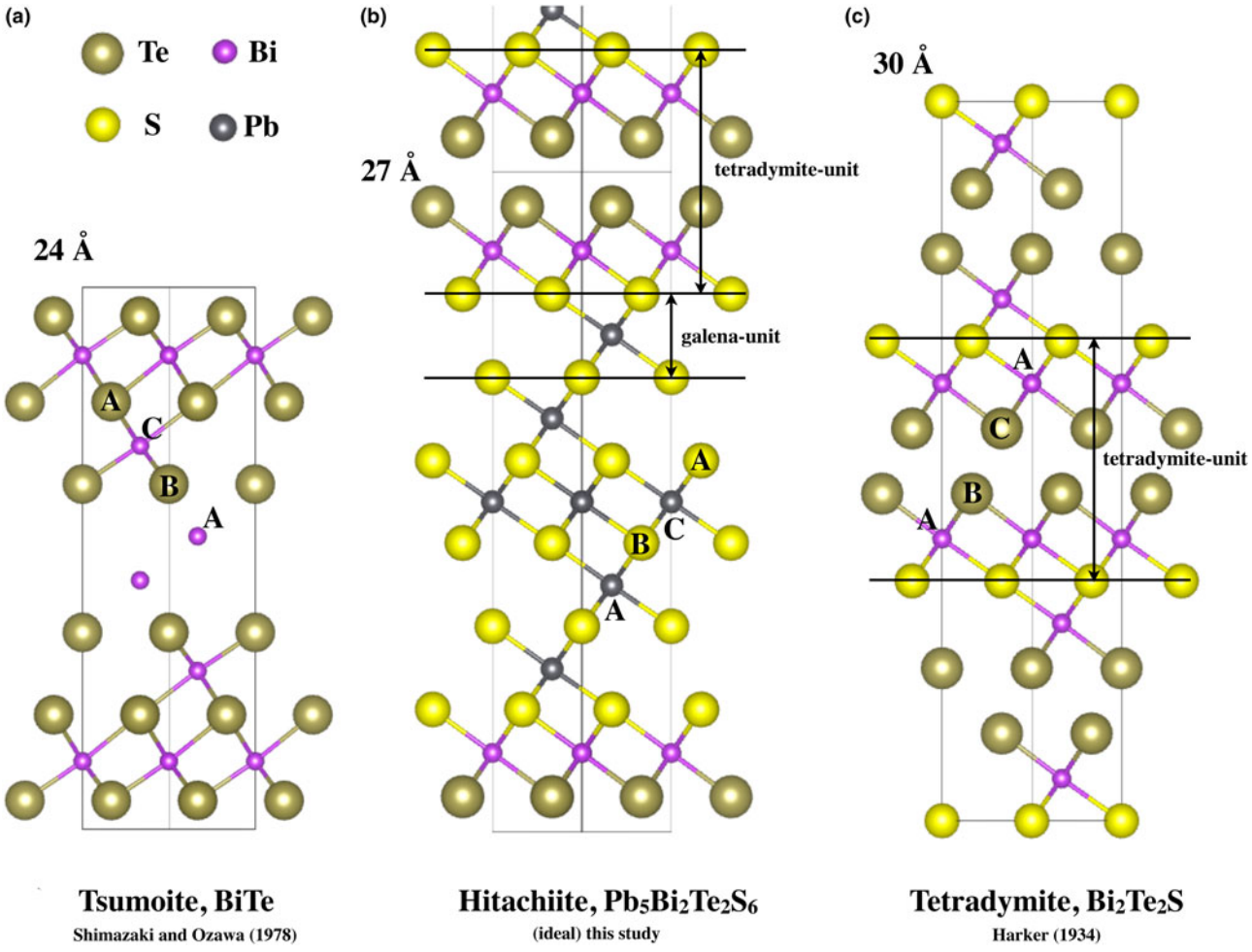

Fig. 5. Crystal structures of hitachiite and related minerals: (*a*) tsumoite, BiTe; (*b*) hitachiite, $Pb_5Bi_2Te_2S_6$; and (*c*) tetradymite, Bi_2Te_2S.

Te–Bi–S), which has an anion–anion interlayer except for S–S (Fig. 5). Other related Pb-bearing minerals with tetradymite archetype structure include rucklidgeite, $PbBi_2Te_4$ (Zhukova and Zaslavskii, 1972) and kochkarite, $PbBi_4Te_7$ (Talybov and Vainshtein, 1962; Shelimova *et al.*, 2004). However, contrary to that, crystal structures of galenobismutite and mozgovaite, $PbBi_4S_7$ are different. These structural differences imply that it is important to consider the role of Se and Te in the structure due to the differences of chemical properties from S.

The chemical formulae of hitachiite, saddlebackite and aleksite lie on the join of Bi_2Te_2S–PbS (Fig. 3*a*). In the review of sulfosalt systematics by Moëlo *et al.* (2008), the aleksite homologous series, $Pb_{(n-1)}Bi_2Ch_{(n+2)}$, are described as layered sulfosalts related to the tetradymite archetype. Hitachiite can be related to this homologous series ($n = 6$). In the case of the originally proposed homologous series of $Pb_nBi_4Te_4S_{n+2}$ (Cook *et al.*, 2007*a*), hitachiite corresponds to the case of $n = 10$. However, the discovery of hitachiite means there are now three species having a similar $Pb_nBi_2Te_2S_{n+1}$ formula with various Pb contents alongside aleksite and saddlebackite. This finding implies that the systematic chemical formulae of these minerals should be expressed alternatively as $Bi_2Te_2S{\cdot}n$PbS (i.e. as a homologous series in the tetradymite–galena join). To fully understand the structural systematics of the minerals within the system Bi_2Te_2S–PbS it is necessary to know their crystal structure.

Based on the idea proposed by Imanov and Semiletov (1971) for the number of layers in complex compounds, Liu and Chang (1994) estimated that the stacking sequence of aleksite was Te–Bi–S–Pb–S–Bi–Te ($Z = 6$) using its *c* periodicity (~79 Å); the stacking sequence of saddlebackite may correspond to Te–Bi–S–Pb–S–Pb–S–Bi–Te ($Z = 2$). With respect to the inner anionic layers of tetradymite archetype structures, Nakajima (1963) suggested that the inner positions of the stacking sequence exhibit more ionic bonding. Similarly, Liu and Chang (1994) pointed out important characteristics of the lead and bismuth chalcogenide with the layer-type structure like tetradymite: (1) PbX_6 octahedral layers form the central part of the unit stacks; (2) PbX_6 octahedra should be regular, and the two *X* layers above and below the Pb layer should show the same composition; and (3) on the basis of the tetradymite structure, if two or more chalcogen elements are present, the smaller one should occupy the inner layer of the unit stacks. The structure of hitachiite seems to satisfy these suggestions.

This homologous series can be structurally characterised by stating that the tetradymite unit (Bi_2Te_2S, S–Bi–Te–Te–Bi–S) sandwiched the galena (S–Pb–S) units by sharing an S layer (Fig. 5). As the details of crystal structures of aleksite ($n = 1$) and saddlebackite ($n = 2$) are still unknown, their structures must await further studies to discern their structural relations. Hitachiite plays an important role in clarifying the structural

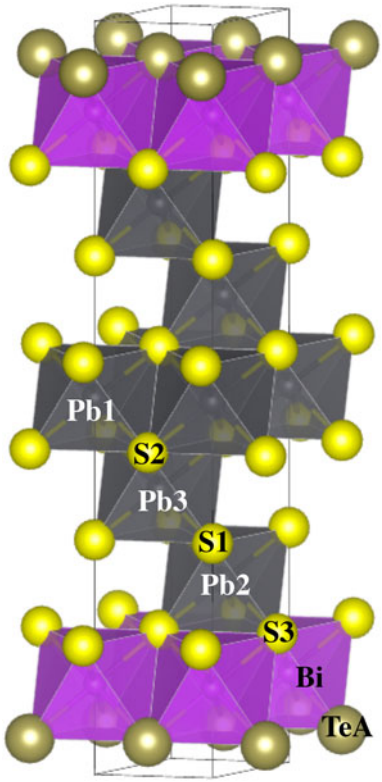

Fig. 6. Ideal structure of hitachiite illustrated using galena-like and tetradymite-like structural units.

systematics of these minerals as for its peculiar distribution of Pb/Bi and Fe in the structure and for the site preference of minor elements such as Fe, Sb and Se.

Acknowledgements. We are grateful to Drs. Leverett, Bindi, and an anonymous reviewer for valuable and constructive comments on revising our manuscript. We sincerely thank Mr. Y. Itoh and Mr. Ohyama of the Technical Division, School of Science, Tohoku University for polishing the sample and making thin sections of hitachiite. This study was partially supported by the Grant of KEK (PAC. No. 2017G137).

Supplementary material. To view supplementary material for this article, please visit https://doi.org/10.1180/mgm.2019.45.

References

Bayliss P. (1991) Crystal chemistry and crystallography of some minerals in the tetradymite group. *American Mineralogist*, **76**, 257–265.

Bindi L. and Cipriani C. (2003) Plumbian baksanite from Tyrnyauz W–Mo deposit, Baksan river valley, northern Caucasus, Russian Federation. *The Canadian Mineralogist*, **41**, 1475–1479.

Cook N.J., Ciobanu C.L., Stanley C.J., Paar W.H. and Sundblad K. (2007*a*) Compositional data for Bi–Pb tellurosulfides. *The Canadian Mineralogist*, **45**, 417–435.

Cook N.J., Ciobanu C.L., Wagner T. and Stanley C.J. (2007*b*) Minerals of the system Bi–Te–Se–S related to the tetradymite archetype. *The Canadian Mineralogist*, **45**, 665–708.

Farrugia L.J. (1999) WinGX suite for small-molecule single-crystal crystallography. *Journal of Applied Crystallography*, **32**, 837–838.

Harker D. (1934) The crystal structure of the mineral tetradymite, Bi_2Te_2S. *Zeit für Kristallographie*, **89**, 175–181.

Imamov P.M. and Semiletov S.A. (1971) The crystal structure of the phases in the system Bi–Se, Bi–Te, and Sb–Te. *Soviet Physics Crystallography*, **15**, 845–850.

Kase K. (1978) Sulfide Minerals of the Hitachi deposits and their comparison with those of the Bessi deposit – studies on sulfide minerals in metamorphosed ores of the Bessi and Hitachi copper deposits (2). *Mining Geology*, **28**, 13–24.

Kase K. and Yamomoto M. (1985) Geochemical study of conformable massive sulfide deposits of the Hitachi mine, Ibaraki Prefecture, Japan. *Mining Geology*, **35**, 17–29.

Kuribayashi T., Nagase T., Nozaki T., Ishibashi J., Shimada K., Shimizu M. and Momma K. (2018) Hitachiite, IMA 2018-027. CNMNC Newsletter No. 44, August 2018, page 1018; *Mineralogical Magazine*, **82**, 1015–1021.

Kuznetsov V.G. and Kanishcheva A.S. (1970) X–ray investigation of alloys of the system Bi_2Te_3–Bi_2S_3. *Inorganic Materials*, **6**, 1113–1116.

Liu H. and Chang L.Y. (1994) Lead and bismuth chalcogenide systems. *American Mineralogist*, **79**, 1159–1166.

Makovicky E. (2006) Crystal structures of sulphides and other chalcogenides. Pp. 7–125 in: *Sulfide Mineralogy and Geochemistry* (D.J. Vaughan, editor). Reviews in Mineralogy and Geochemistry, 61. Mineralogical Society of America and the Geochemical Society, Chantilly, Virginia, USA.

Moëlo Y., Makovicky E., Mozgova N.N., Jambor J.L., Cook N., Pring A., Paar W., Nickel E.H., Graeser S., Karup–Moøller S., Balic–Žunic T., Mumme W.G., Vurro F., Topa D., Bindi L., Bente K. and Shimizu M. (2008) Sulfosalt systematics: a review. Report of sulfosalt sub-committee of the IMA commission on ore mineralogy. *European Journal of Mineralogy*, **20**, 7–46.

Momma K. and Izumi F. (2011) VESTA 3 for three-dimensional visualization of crystals, volumetric and morphology data. *Journal of Applied Crystallography*, **44**, 1272–1276.

Nakajima S. (1963) The crystal structure of $Bi_2Te_{3-x}Se_x$. *Journal of Physics and Chemistry of Solids*, **24**, 479–485.

Nakamuta Y. (1999) Precise analysis of a very small mineral by an X–ray diffraction method. *Journal of the Mineralogical Society of Japan*, **28**, 117–121 [in Japanese with English abstract].

Noda Y., Masumoto K., Ohba S., Saito Y., Toriumi K., Iwata Y. and Shibuya I. (1987) Temperature dependence of atomic thermal parameters of lead chalcogenides, PbS, PbSe and PbTe. *Acta Crystallographica*, **C43**, 1443–1445.

Nozaki T., Kato Y. and Suzuki K. (2014) Re–Os geochronology of the Hitachi volcanic massive sulfide deposit: The oldest ore deposit in Japan. *Economic Geology*, **109**, 2023–2034.

Oszlanyi G. and Suto A. (2004) Ab initio structure solution by charge flipping, *Acta Crystallographica*, **A60**, 134–141.

Palatinus L. and Chapuis G. (2007) SUPERFLIP – a computer program for the solution of crystal structures by charge flipping in arbitrary dimensions. *Journal of Applied Crystallography*, **40**, 456–462.

Parkin S.Moezzi B. and Hope H. (1995) XABS2: an empirical absorption correction program. *Journal of Applied Crystallography*, **28**, 53–56.

Pauling L. (1975) The formula, structure and chemical bonding of tetradymite $Bi_{14}Te_{13}S_8$–$Bi_{14}Te_{15}S_6$. *American Mineralogist*, **60**, 994–997.

Prince E. (editor) (2004) *International Tables for X–ray Crystallography. Volume C: Mathematical, Physical and Chemical Tables*. 3rd edition. International Union of Crystallography. Kluwer Academic Publisher, Dordrecht, Netherlands.

Sheldrick G.M. and Schneider T.R. (1997) SHELXL: high–resolution refinement. *Methods in Enzymology*, **277**, 319–343.

Shelimova L.E., Karpinski O.G, Svechnikova T.E., Avilov E.S., Kretova M.A. and Zemskov V.S. (2004) Synthesis and structure of layered compounds in the PbTe–Bi_2Te_3 and PbTe–Sb_2Te_3 systems. *Inorganic Materials*, **40**, 1264–1270.

Shimazaki H. and Ozawa T. (1978) Tsumoite, BiTe, a new mineral from the Tsumo mine, Japan. *American Mineralogist*, **63**, 1162–1165.

Strunz H. and Nickel E.H. (2001) Class 2. SULFIDES and SULFOSALTS. pp. 56–147 in: *Strunz Mineralogical Tables 9th Edition*. E. Schweizerbart'sche Verlagsbuchhandlung (Nägele u. Obermiller), Stuttgart, Germany.

Tagiri M., Dunkley D.J., Adachi T., Hiroi Y. and Fanning C.M. (2011) SHRIMP dating of magmatism in the Hitachi metamorphic terrane, Abukuma Belt, Japan: Evidence for a Cambrian volcanic arc. *Island Arc*, **20**, 259–279.

Talybov A.G. and Vainshtein B.K. (1962) An electron diffraction study of the second superlattice in $PbBi_4Te_7$. *Kristallografiya*, **7**, 43–50.

Zhukova T.B. and Zaslavskii A.I. (1972) Crystal structures of the compounds $PbBi_4Te_7$ $PbBi_2Te_4$ $SnBi_4Te_7$ $SnBi_2Te_4$ $SnSb_2Te_4$ and $GeBi_4Te_7$. *Kristallografiya*, **16**, 918–922.